PERGAMON

International Journal of Solids and Structures 37 (2000) 5943–5955

INTERNATIONAL JOURNAL OF SOLIDS and STRUCTURES

www.elsevier.com/locate/ijsolstr

On the elastic axisymmetric deformation of a rod containing a single cylindrical inclusion

Z. Zhong[a], Q.P. Sun[b,*], P. Tong[b]

[a]*Department of Engineering Mechanics and Technology, Tongji University, Shanghai 200092, People's Republic of China*
[b]*Department of Mechanical Engineering, The Hong Kong University of Science and Technology, Clear Water Bay, Kowloon, Hong Kong SAR, P.R. China*

Received 19 February 1999; in revised form 17 June 1999

Abstract

This paper studies the axisymmetric deformation of a rod containing a single cylindrical transformation inclusion with uniform axisymmetric eigenstrain. Elastic solutions of the problem are obtained by means of the principle of superposition. The original problem is divided into two sub-problems to derive the analytical expressions for the displacements, the stresses and the elastic strain energy of the whole rod. Quantitative pictures on the stress and strain jumps across the inclusion–matrix interface and on the evolution of the strain energy of the whole rod are illustrated. The results show that the normalized elastic strain energy depends on the relative length of the cylindrical inclusion for the length–radius ratio $l/a < 2$. This strain energy increases very quickly at the initial growth and soon reaches the peak value, then decreases with the further increase of l/a and finally reaches its steady state value. Several deformation features of this non-classical inclusion–matrix system are discussed. The work of this paper also provides a quantitative solution in the investigation of the propagation of strain discontinuity observed during thermoelastic phase transformation in solids such as TiNi shape memory alloy wires.

Keywords: Elastic rod; Cylindrical inclusion; Eigenstrain; Axisymmetric deformation

1. Introduction

Experimental results on tensile test of NiTi Shape Memory Alloy (SMA) wires and strips in recent years have demonstrated that the deformation in the superelastic region is realized by the reversible propagation of single or several martensite bands during the forward and reverse transformations (see

* Corresponding author. Tel.: +852-2358-8655; fax: +852-2358-1543.
E-mail address: meqpsun@usthk.ust.hk (Q.P. Sun).

0020-7683/00/$ - see front matter
PII: S0020-7683(99)00269-3

Lin et al., 1994, 1996; Shaw and Kyriakides, 1995, 1997, 1998). In addition to this general feature, there is a strong thermal and mechanical interaction in the response of the specimen because of the latent heat of the transformation. However, it is interesting to note that in some Cu-based systems (such as CuZnAl and CuAlBe polycrystalline SMAs) the tensile stress–strain curves at superelasticity are normally stable and monotonic and, therefore, the deformation is macroscopically homogeneous (see Patoor et al., 1996). In order to understand and model the band propagation phenomena and to explain such dramatic difference in the deformation modes in the same superelastic regimes, the physical underlying mechanisms must be explored. At the same time, from continuum mechanics point of view, the following two questions should be answered: (1) How, why, and when do such strain discontinuity happen in an initially uniformly stressed and deformed body? (2) What is the overall response of the TiNi tensile specimen and its dependence on the kinematical factors (such as the transformation strain, the interface property, the number of interfaces and the geometry of the specimen) if such a deformation mode (i.e., via propagation of strain discontinuity) is prescribed under external thermomechanical loading.

Without doubt, the elastic stress strain fields and strain energy distribution in the specimen and their evolution play very important role because of the thermoelastic nature of martensitic transformation in shape memory alloys. Since the transformation process is accomplished by the growth of martensite bands, a special type of inclusion–matrix system is used to model the SMA wire specimen containing a transformation band. The observed propagation of the band can be simulated by a growing inclusion in the cylindrical rod. Though a great amount of work has been done on the traditional matrix–inclusion problems such as those in mechanics of composite materials and polycrystals, few analytical solutions are available in the literature for this special type of non-classic inclusion–matrix system.

As a part of an attempt to understand and model the phenomenon described above, this paper aims providing an elastic solution of the rod. In Section 2, the basic equations and boundary conditions for this inclusion–matrix system are described. In Section 3, solution techniques to determine the stress and displacement fields as well as the strain energy of the rod are formulated. The obtained results and their implications to the transformation behavior of shape memory alloys are discussed in Section 4.

2. Problem formulation and basic equations

Consider an infinitely long cylindrical rod with a circular cross section of radius a as shown in Fig. 1. The rod contains a segment Ω of height l with uniform axisymmetric eigenstrain ε_{ij}^* (due to phase transformation or other sources). The elastic constants of the domain are assumed to be the same as the remaining matrix (note: in real martensitic transformation in SMA, the Young's modulus of martensite is less than that of austenite, then it will be treated as an inhomogeneous inclusion problem). The eigenstrain causes a nonuniform deformation and internal stress in the rod. In order to analyze the present problem, a cylindrical coordinate system (r, θ, z) is introduced, with the z-axis being along the cylindrical axis, as depicted in Fig. 1. Since the eigenstrain ε_{ij}^* is axisymmetric with respect to z-axis and distributes uniformly in the inclusion Ω, its nonzero components can be written as

$$\varepsilon_r^* = \varepsilon_\theta^* = \varepsilon_1^* \quad \varepsilon_z^* = \varepsilon_2^* \tag{1}$$

In the cylindrical coordinates r, θ, z, the displacement component u_θ vanishes and u_r, u_z are independent of θ. The nonzero strain components ε_r, ε_θ, ε_z and γ_{rz} are calculated by the following strain-displacement relations

$$\varepsilon_r = \frac{\partial u_r}{\partial r} \quad \varepsilon_\theta = \frac{u_r}{r} \quad \varepsilon_z = \frac{\partial u_z}{\partial z} \quad \gamma_{rz} = \frac{\partial u_r}{\partial z} + \frac{\partial u_z}{\partial r} \tag{2}$$

The corresponding stress components σ_r, σ_θ, σ_z and τ_{rz} in the inclusion ($|z| < l/2, r < a$) can be calculated through the constitutive relations:

$$\sigma_r = \frac{E}{1+\nu}\left[\frac{\nu}{1-2\nu}(\theta - \theta^*) + \left(\varepsilon_r - \varepsilon_r^*\right)\right]$$

$$\sigma_\theta = \frac{E}{1+\nu}\left[\frac{\nu}{1-2\nu}(\theta - \theta^*) + \left(\varepsilon_\theta - \varepsilon_\theta^*\right)\right]$$

$$\sigma_z = \frac{E}{1+\nu}\left[\frac{\nu}{1-2\nu}(\theta - \theta^*) + \left(\varepsilon_z - \varepsilon_z^*\right)\right]$$

$$\tau_{rz} = \frac{E}{2(1+\nu)}\gamma_{rz} \tag{3}$$

while their counterparts in the matrix ($|z| > l/2, r < a$) are obtained as

$$\sigma_r = \frac{E}{1+\nu}\left(\frac{\nu}{1-2\nu}\theta + \varepsilon_r\right)$$

$$\sigma_\theta = \frac{E}{1+\nu}\left(\frac{\nu}{1-2\nu}\theta + \varepsilon_\theta\right)$$

$$\sigma_z = \frac{E}{1+\nu}\left(\frac{\nu}{1-2\nu}\theta + \varepsilon_z\right)$$

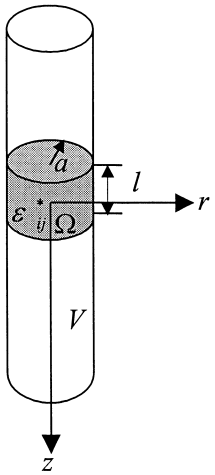

Fig. 1. A schematic of a cylindrical rod with an inclusion.

$$\tau_{rz} = \frac{E}{2(1+\nu)}\gamma_{rz} \tag{4}$$

where $\theta = \varepsilon_r + \varepsilon_\theta + \varepsilon_z$, $\theta^* = \varepsilon_r^* + \varepsilon_\theta^* + \varepsilon_z^*$, and E and ν are Young's modulus and Poisson's ratio, respectively. Furthermore, the stress components in the inclusion and the matrix satisfy the following equations of equilibrium:

$$\frac{\partial \sigma_r}{\partial r} + \frac{\partial \tau_{rz}}{\partial z} + \frac{\sigma_r - \sigma_\theta}{r} = 0$$

$$\frac{\partial \tau_{rz}}{\partial r} + \frac{\partial \sigma_z}{\partial z} + \frac{\tau_{rz}}{r} = 0 \tag{5}$$

Substituting Eqs. (2)–(4) into Eq. (5), we obtain the Navier equations for the displacements:

$$\frac{1}{1-2\nu}\frac{\partial \theta}{\partial r} + \nabla^2 u_r - \frac{u_r}{r^2} = 0$$

$$\frac{1}{1-2\nu}\frac{\partial \theta}{\partial z} + \nabla^2 u_z = 0 \tag{6}$$

where

$$\nabla^2 = \frac{\partial^2}{\partial r^2} + \frac{1}{r}\frac{\partial}{\partial r} + \frac{\partial^2}{\partial z^2}.$$

The stress-free boundary conditions at the lateral surface ($r = a$) are

$$\sigma_r = \tau_{rz} = 0 \quad (r = a). \tag{7}$$

The continuity conditions for the traction and the displacements at the interface between the inclusion and the matrix require that the displacements u_r, u_z and the stresses σ_z, τ_{rz} be continuous at the interfaces $z = l/2$ and $z = -l/2$. The traction-free end conditions at the ends of the infinite cylindrical rod can be written as

$$\sigma_z = \tau_{rz} = 0 \quad |z| \to \infty \tag{8}$$

In the following sections, the deformation and the stress field in the rod will be determined using the basic equations and boundary conditions above.

3. Solution

3.1. Decomposition of the problem

According to the principle of superposition, the original problem can be decomposed into two sub-problems.

3.1.1. Sub-problem I

The displacements of the cylindrical rod have the following forms

$$u_r^{\mathrm{I}} = 0 \quad u_z^{\mathrm{I}} = Az \quad \left(|z| < \frac{l}{2}, r < a\right)$$

$$u_r^{\mathrm{I}} = 0 \quad u_z^{\mathrm{I}} = -A\frac{l}{2} \quad \left(z < -\frac{l}{2}, r < a\right)$$

$$u_r^{\mathrm{I}} = 0 \quad u_z^{\mathrm{I}} = A\frac{l}{2} \quad \left(z > \frac{l}{2}, r < a\right) \tag{9}$$

with

$$A = \frac{2\nu}{1-\nu}\varepsilon_1^* + \varepsilon_2^* \tag{10}$$

Accordingly the stresses in the rod are obtained through (3) and (4) as

$$\sigma_r^{\mathrm{I}} = \sigma_\theta^{\mathrm{I}} = -\frac{E}{1-\nu}\varepsilon_1^* \quad \sigma_z^{\mathrm{I}} = \tau_{rz}^{\mathrm{I}} = 0 \left(|z| < \frac{l}{2}, r < a\right)$$

$$\sigma_r^{\mathrm{I}} = \sigma_\theta^{\mathrm{I}} = \sigma_z^{\mathrm{I}} = \tau_{rz}^{\mathrm{I}} = 0 \quad \left(|z| > \frac{l}{2}, r < a\right) \tag{11}$$

It is easy to check that the displacement solution as given in Eq. (9) automatically satisfies the governing equation (6), the remote boundary condition (8), as well as the continuity conditions for the traction and the displacement at the interface between the inclusion and the matrix. Unfortunately, the solution does not satisfy the lateral boundary condition (7) for $|z| < l/2$. At the boundary $r = a$, the solution gives

$$\sigma_r^{\mathrm{I}}|_{r=a} = p = -\frac{E}{1-\nu}\varepsilon_1^* \quad \tau_{rz}^{\mathrm{I}}|_{r=a} = 0 \quad \left(|z| < \frac{l}{2}\right)$$

$$\sigma_r^{\mathrm{I}}|_{r=a} = \tau_{rz}^{\mathrm{I}}|_{r=a} = 0 \quad \left(|z| > \frac{l}{2}\right) \tag{12}$$

In order to satisfy the boundary condition (7), an auxiliary solution is superimposed, which will be defined in Section 3.1.2.

3.1.2. Sub-problem II

The same infinitely long cylindrical rod is subjected to a distributed pressure $-p$ over $|z| < l/2$ as shown in Fig. 2. The basic equations and the boundary conditions at remote ends are given by Eqs. (2), (4)–(6) and (8), while the lateral boundary conditions can be described as

$$\sigma_r^{\mathrm{II}}|_{r=a} = -p \quad \tau_{rz}^{\mathrm{II}}|_{r=a} = 0 \quad \left(|z| < \frac{l}{2}\right)$$

$$\sigma_r^{\mathrm{II}}|_{r=a} = \tau_{rz}^{\mathrm{II}}|_{r=a} = 0 \left(|z| > \frac{l}{2}\right) \tag{13}$$

where

$$p = -\frac{E}{1-\nu}\varepsilon_1^* \tag{14}$$

To obtain the solution, a stress function ϕ is introduced. The stress components are given by

$$\sigma_r^{II} = \frac{\partial}{\partial z}\left(\nu\nabla^2\phi - \frac{\partial^2\phi}{\partial r^2}\right)$$

$$\sigma_\theta^{II} = \frac{\partial}{\partial z}\left(\nu\nabla^2\phi - \frac{1}{r}\frac{\partial\phi}{\partial r}\right)$$

$$\sigma_z^{II} = \frac{\partial}{\partial z}\left((2-\nu)\nabla^2\phi - \frac{\partial^2\phi}{\partial z^2}\right)$$

$$\tau_{rz}^{II} = \frac{\partial}{\partial r}\left((1-\nu)\nabla^2\phi - \frac{\partial^2\phi}{\partial z^2}\right) \tag{15}$$

where ϕ satisfies the bi-harmonic equation

$$\nabla^2\nabla^2\phi = 0 \tag{16}$$

Accordingly, the displacements can be expressed as (see Timoshenko and Goodier, 1970)

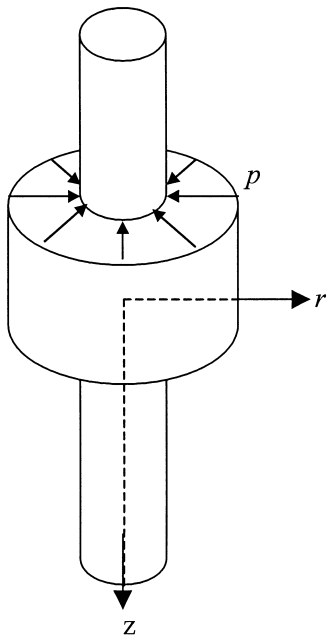

Fig. 2. A schematic of a cylindrical rod subjected to a distributed pressure p.

$$u_r^{\mathrm{II}} = -\frac{1+\nu}{E}\frac{\partial^2\phi}{\partial r\partial z}$$

$$u_z^{\mathrm{II}} = \frac{1+\nu}{E}\left[2(1-\nu)\nabla^2\phi - \frac{\partial^2\phi}{\partial z^2}\right] \tag{17}$$

Hence the problem is reduced to the determination of the stress function ϕ with boundary conditions (8) and (13), which will be given in Section 3.2.

By superposing the solutions of sub-problems I and II, we obtain the total displacements and stresses

$$u_r = u_r^{\mathrm{I}} + u_r^{\mathrm{II}} \qquad u_z = u_z^{\mathrm{I}} + u_z^{\mathrm{II}}$$

$$\sigma_r = \sigma_r^{\mathrm{I}} + \sigma_r^{\mathrm{II}} \qquad \sigma_\theta = \sigma_\theta^{\mathrm{I}} + \sigma_\theta^{\mathrm{II}}$$

$$\sigma_z = \sigma_z^{\mathrm{I}} + \sigma_z^{\mathrm{II}} \qquad \tau_{rz} = \tau_{rz}^{\mathrm{I}} + \tau_{rz}^{\mathrm{II}} \tag{18}$$

which satisfy the basic equations and boundary conditions of the original problem described in Section 2.

3.2. Solution of sub-problem II

Assuming the stress function ϕ as

$$\phi = 2\int_0^\infty \left[\rho(k)I_0(kr) - krI_1(kr)\right]f(k)\sin kz\sin\frac{kl}{2}\,\mathrm{d}k \tag{19}$$

where $I_0(kr)$ and $I_1(kr)$ are the modified Bessel functions of zero order and first order, respectively. Functions $\rho(k)$ and $f(k)$ will be determined later. It is easy to verify that this form of stress function satisfies Eq. (16).

From Eqs. (17) and (15), we obtain the corresponding displacements and stresses as

$$u_r^{\mathrm{II}} = \frac{2(1+\nu)}{E}\int_0^\infty \left[krI_0(kr) - \rho(k)I_1(kr)\right]k^2f(k)\cos kz\sin\frac{kl}{2}\,\mathrm{d}k$$

$$u_z^{\mathrm{II}} = \frac{2(1+\nu)}{E}\int_0^\infty \left\{\left[\rho(k) - 4(1-\nu)\right]I_0(kr) - krI_1(kr)\right\}k^2f(k)\sin kz\sin\frac{kl}{2}\,\mathrm{d}k \tag{20}$$

and

$$\sigma_r^{\mathrm{II}} = 2\int_0^\infty \left\{\left[1-2\nu-\rho(k)\right]I_0(kr) + \left[kr + \frac{\rho(k)}{kr}\right]I_1(kr)\right\}k^3f(k)\cos kz\sin\frac{kl}{2}\,\mathrm{d}k$$

$$\sigma_\theta^{\mathrm{II}} = 2\int_0^\infty \left[(1-2\nu)I_0(kr) - \frac{\rho(k)}{kr}I_1(kr)\right]k^3f(k)\cos kz\sin\frac{kl}{2}\,\mathrm{d}k$$

$$\sigma_z^{\mathrm{II}} = 2\int_0^\infty \left\{\left[\rho(k) - 2(2-\nu)\right]I_0(kr) - krI_1(kr)\right\}k^3f(k)\cos kz\sin\frac{kl}{2}\,\mathrm{d}k$$

$$\tau_{rz}^{\mathrm{II}} = 2\int_0^\infty \left\{\left[\rho(k) - 2(1-\nu)\right]I_1(kr) - krI_0(kr)\right\}k^3 f(k)\sin kz \sin\frac{kl}{2}\,\mathrm{d}k \tag{21}$$

In order to satisfy boundary condition (13) functions $\rho(k)$ and $f(k)$ should be chosen as

$$\rho(k) = 2(1-\nu) + ka\frac{I_0(ka)}{I_1(ka)} \tag{22}$$

$$f(k) = -\frac{p}{\pi k^4}\left\{\left[1-2\nu-\rho(k)\right]I_0(ka) + \left[ka + \frac{\rho(k)}{ka}\right]I_1(ka)\right\}^{-1} \tag{23}$$

In the derivation of $f(k)$ the following integration formula is used:

$$\int_0^\infty \frac{\cos kz}{k}\sin\frac{kl}{2}\,\mathrm{d}k = \begin{cases} \dfrac{\pi}{2} & \text{for } |z| < l/2 \\ 0 & \text{for } |z| > l/2 \end{cases} \tag{24}$$

It is easy to check that σ_z^{II} and τ_{rz}^{II} satisfy the stress-free boundary conditions at infinity in the sense of Saint-Venant's principle, i.e., $\int_s \sigma_z^{\mathrm{II}}\,\mathrm{d}s = 0$ and $\int_s \tau_{rz}^{\mathrm{II}}\,\mathrm{d}s = 0$, where s denotes the cross section.

A similar solution technique for such a problem was described in the book of Timoshenko and Goodier (1970). The present approach is more direct and simple.

3.3. Elastic strain energy

The total elastic strain energy W of the rod can be calculated as (Mura, 1987)

$$W = \frac{1}{2}\int_V \sigma_{ij}\varepsilon_{ij}^{\mathrm{e}}\,\mathrm{d}V = -\frac{1}{2}\left[(\bar{\sigma}_r + \bar{\sigma}_\theta)\varepsilon_1^* + \bar{\sigma}_z\varepsilon_2^*\right]V_\Omega \tag{25}$$

where V is the entire domain of the rod and $V_\Omega(=\pi a^2 l)$ represents the volume of the inclusion, $\varepsilon_{ij}^{\mathrm{e}}$ is the elastic strain, and $\bar{\sigma}_r$, $\bar{\sigma}_\theta$ and $\bar{\sigma}_z$ denote the average of stresses σ_r, σ_θ and σ_z over the inclusion Ω

$$\bar{\sigma}_r = \frac{1}{V_\Omega}\int_\Omega \sigma_r\,\mathrm{d}V \quad \bar{\sigma}_\theta = \frac{1}{V_\Omega}\int_\Omega \sigma_\theta\,\mathrm{d}V \quad \bar{\sigma}_z = \frac{1}{V_\Omega}\int_\Omega \sigma_z\,\mathrm{d}V \tag{26}$$

Eqs. (11), (15) and (18) give

$$\bar{\sigma}_r + \bar{\sigma}_\theta = -\frac{2E\varepsilon_1^*}{1-\nu}H\left(\frac{l}{a},\nu\right) \quad \bar{\sigma}_z = 0 \tag{27}$$

where

$$H\left(\frac{l}{a},\nu\right) = 1 + \int_0^\infty G(t)\left(\sin\frac{tl}{2a}\right)^2\,\mathrm{d}t \tag{28}$$

with

$$G(t) = \frac{8a(1+\nu)}{\pi l t^3}\left\{\left[1-2\nu-\rho(t)\right]\frac{I_0(t)}{I_1(t)} + t + \frac{\rho(t)}{t}\right\}^{-1} \tag{29}$$

$$\rho(t) = 2(1-\nu) + t\frac{I_0(t)}{I_1(t)} \tag{30}$$

The elastic strain energy of the rod can be rewritten as

$$W = \frac{\pi a^2 l}{1-\nu} H\left(\frac{l}{a}, \nu\right) E\left(\varepsilon_1^*\right)^2 \tag{31}$$

For a given a, ν, E, ε_1^*, W is a function of l only. Comparing with the elastic strain energy expression of an ellipsoidal inclusion in an infinite domain (Eshelby, 1957; Mura, 1987)

$$W = -\frac{1}{2} V_\Omega \sigma_{ij} \varepsilon_{ij}^* = -\frac{1}{2} V_\Omega C_{ijkl}(S_{klmn} - I_{klmn}) \varepsilon_{mn}^* \varepsilon_{ij}^*, \tag{32}$$

One sees that both expressions are very similar. The coefficient $\frac{H(l/a,\ \nu)}{(1-\nu)}$ in Eq. (31) serves as the shape factor of the cylindrical inclusion (like S_{ijkl} for ellipsoids).

4. Discussion and conclusions

4.1. The stress field distribution and evolution

The stress field distribution and evolution have the following features: (1) The axial component of eigenstrain ε_z^* has no contribution to the stress and the total elastic strain energy of the rod. It induces

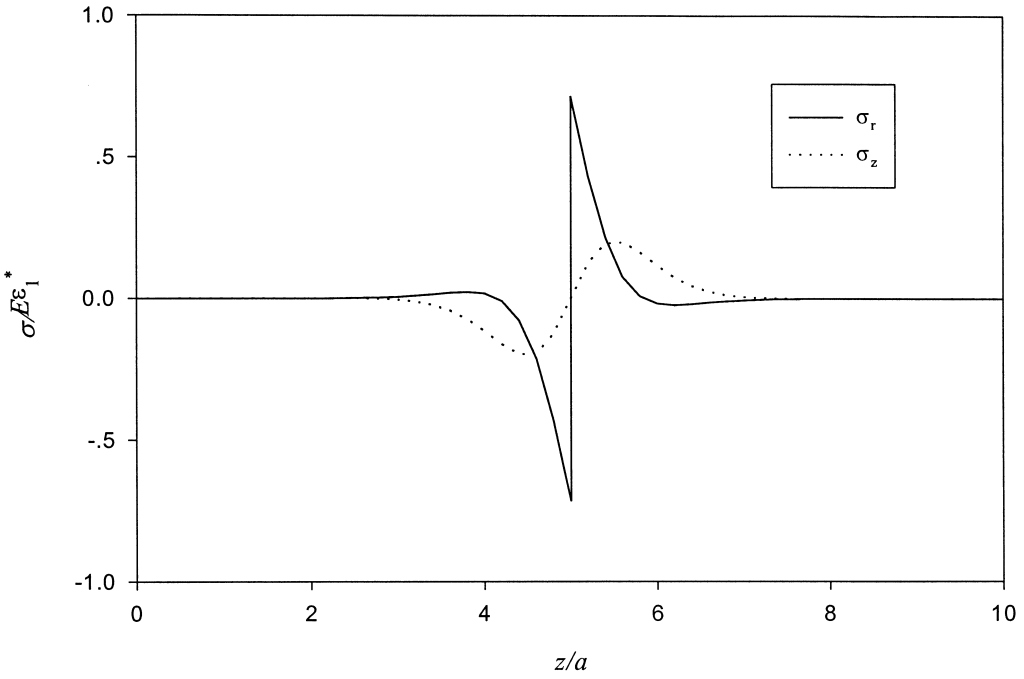

Fig. 3. The variation of stresses σ_r and σ_z normalized by $E\varepsilon_1^*$ along the positive z-axis when $l = 10a$ and $\nu = 0.3$.

only an axial displacement of the rod. (2) Fig. 3 shows the variation of stresses σ_r and σ_z (normalized by $E\varepsilon_1^*$) along the positive z-axis (for $r = 0$, $z \geq 0$, we have $\sigma_r = \sigma_\theta$ and $\tau_{rz} = 0$) for $l = 10a$ and $\nu = 0.3$. Several typical features of the stress distribution can be identified. Both σ_r and σ_z concentrate near the interface ($z = 5a$) and decrease rapidly to zero away from the interface. The stress σ_r has a jump across the interface while σ_z is still continuous across the interface. For $l \geq 5a$, there is little interaction between the stress fields of the two interfaces. When the two interfaces come closer, the interaction of the stress fields becomes obvious. Fig. 4 shows the variation of stresses σ_r and σ_z (normalized by $E\varepsilon_1^*$) along the positive z-axis for the case $l = 2a$ and $\nu = 0.3$. It is seen that the stresses in the center part of the inclusion do not vanish because of this interaction and σ_r increases as the two interfaces approach each other (see Fig. 5).

4.2. Implications to the transformation behavior of a SMA wire or rod

Fig. 6 shows the variation of the normalized elastic strain energy $W^*(= W/a^3 E\varepsilon_1^{*2})$ of the rod as a function of the normalized length of the inclusion l/a ($\nu = 0.3$). The normalized elastic strain energy increases monotonically and very quickly reaches a peak value as the inclusion grows. Further growth of the inclusion causes a decrease in strain energy and finally reaches a steady state value for $l/a > 2$.

This type of energy evolution with the growth of transformation band has very important implications. Based on the thermodynamic analysis of the matrix–inclusion system with energy dissipation during transformation, an inclusion theory for the propagation of martensite band can be established (Sun and Zhong, 1999). The basic idea of this theory is as follows: once we know the expression of the elastic strain energy of the rod, we can construct the free energy expression of the

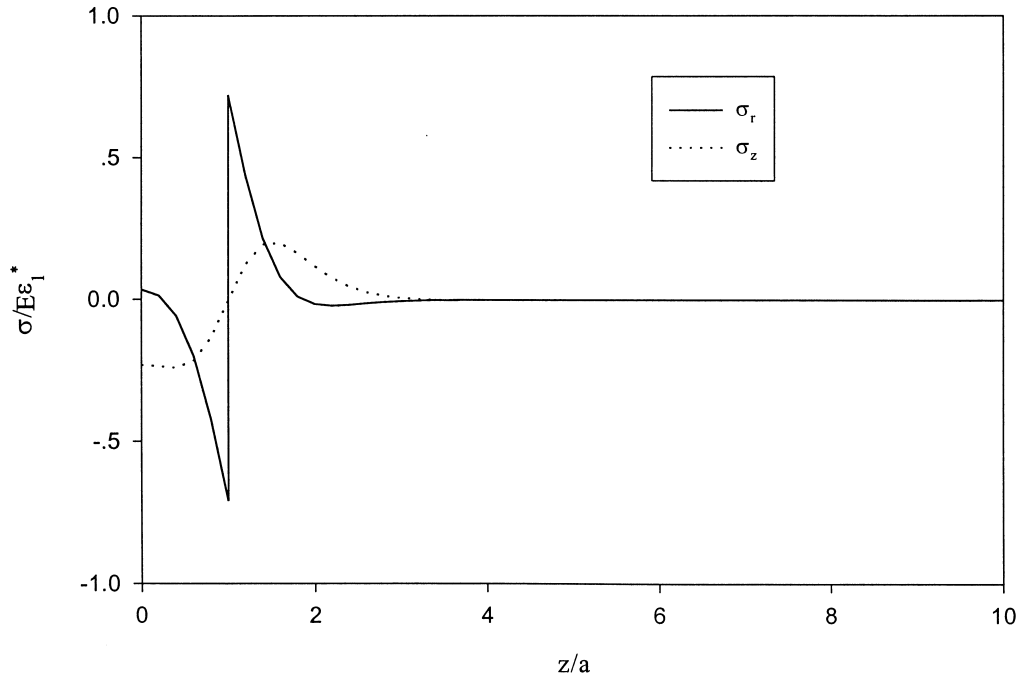

Fig. 4. The variation of stresses σ_r and σ_z normalized by $E\varepsilon_1^*$ along the positive z-axis when $l = 2a$ and $\nu = 0.3$.

matrix–inclusion system during transformation where the band length l is naturally identified as the internal variable of the system. The transformation condition and the evolution rule for the increase and decrease of the band in the stress–temperature space can be derived. According to this theory, the nucleation and initial growth of martensitic band requires much higher stress than the subsequent propagation. From the obtained force–displacement relations of the rod during propagation of the inclusion, the nominal stress–strain relations of the rod for different length of the specimen can be calculated. The obtained theoretical predictions do quantitatively capture the observed deformation features of the rod as reported in the test. The readers are referred to Sun and Zhong (1999) for detailed derivation and discussion.

4.3. Several discussions on this simplified matrix–inclusion model

It should be recognized that the inclusion–matrix system developed in this paper is a simplified model. For example: the macroscopic observed band propagation in a wire specimen is modeled as a growing cylindrical inclusion; the A–M interface is assumed to be perpendicular to the loading axis, and the macroscopic transformation strain in the band (resulted from the volume average of the transformation strains in all grains of bulk polycrystal) is taken as a material constant (this assumption is deduced from the experimental observation (Shaw and Kyriakides, 1995)). As a result of this simplification the details on the microscopic level are neglected (such as the orientation distribution of the habit planes in the grains of a polycrystalline SMA; the rapid but continuous change of volume fraction of martensite across the front etc.). Since the interest is on the macroscopic response, it is believed that such a macroscopic simplified modeling can reveal and characterize the main deformation features of the transformation process that involves the martensite band propagation at the same macroscopic level.

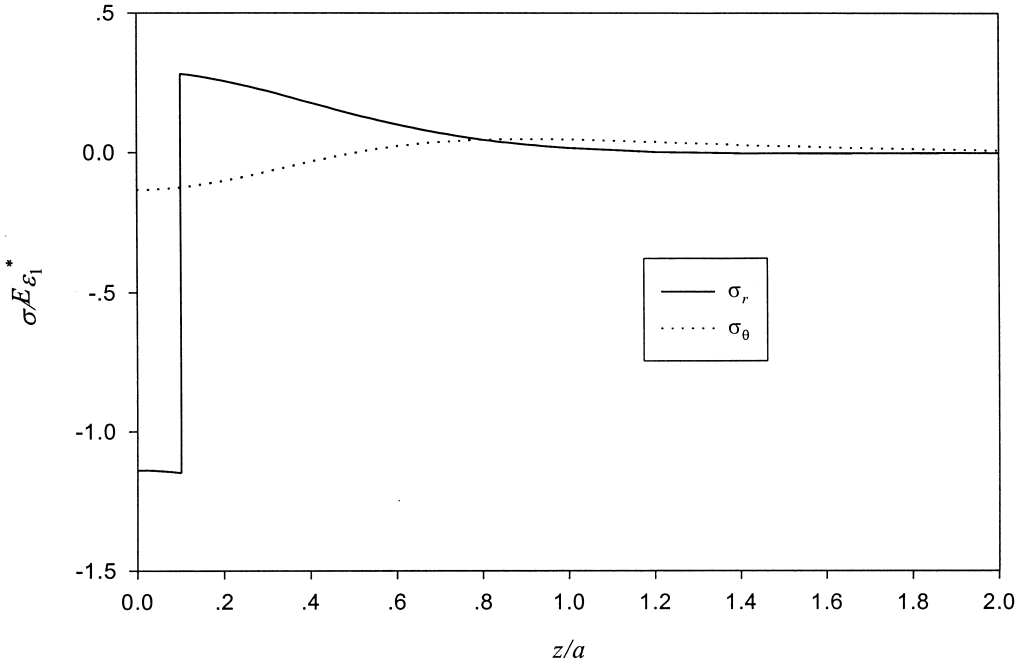

Fig. 5. The variation of stresses σ_r and σ_z normalized by $E\varepsilon_1^*$ along the positive z-axis when $l = 0.2a$ and $\nu = 0.3$.

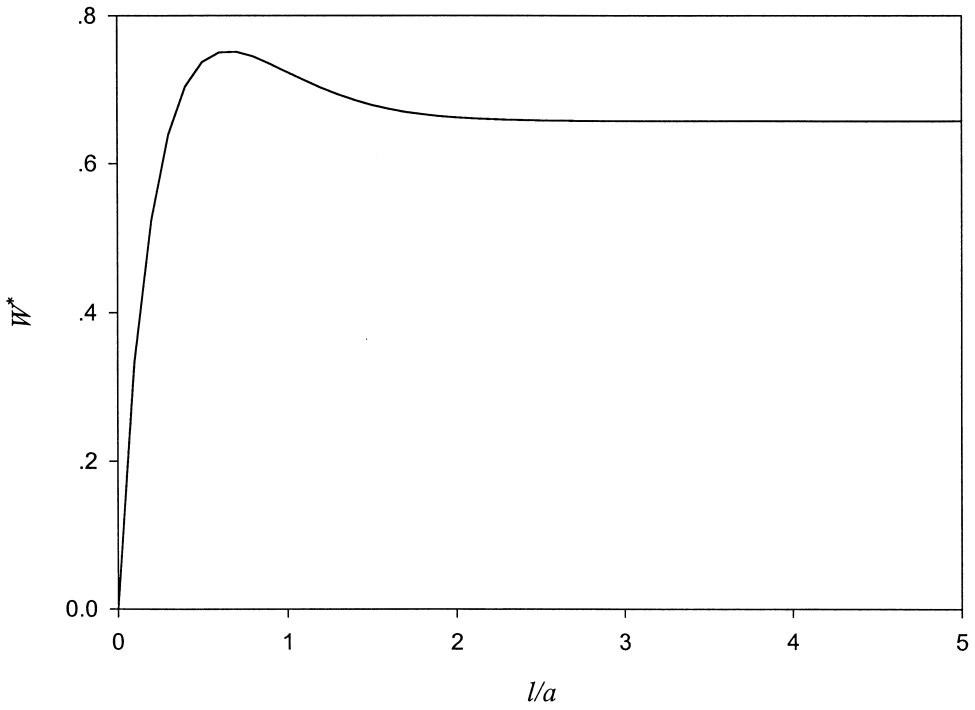

Fig. 6. The variation of the normalized elastic strain energy W^* vs. the normalized height of the inclusion l/a for the case of $\nu = 0.3$.

Certainly, the effect of the A–M interface orientation as well as the difference in the modulus between the austenite and austenite must be further incorporated into the model if a direct quantitative comparison with the test data of a real NiTi polycrystal are to be made.

Acknowledgements

The reported work was performed with the financial support of the Research Grant Council of Hong Kong SAR of China (Project no. HKUST 6037/98E), the National Natural Science Foundation of China, the National Excellent Young Scholar Foundation of China (Project no. 19825107).

References

Eshelby, J.D., 1957. The determination of the elastic field of an ellipsoidal inclusion and related problems. Proc. R. Soc. A 241, 376–396.

Lin, P.H., Tobushi, H., Tanaka, K., Hattori, T., Makita, M., 1994. Pseudoelastic behaviour of TiNi shape memory alloy subjected to strain variations. J. Intell. Mater. Syst. Struct. 5, 694–701.

Lin, P.H., Tobushi, H., Tanaka, K., Ikai, A., 1996. Deformation properties of TiNi shape memory alloy. JSME Int. J. A39, 108–116.

Mura, T., 1987. Micromechanics of Defects in Solids, 2nd revised ed. Martinus Nijhoff, Dordrecht.

Patoor, E., Eberhardt, A., Berveiller, M., 1996. Micromechanical modeling of superelasticity in shape memory alloys. J. Phys. IV 6, C1-277–C1-292.

Shaw, J.A., Kyriakides, S., 1995. Thermomechanical aspects of NiTi. J. Mech. Phys. Solids 43, 1243–1281.

Shaw, J.A., Kyriakides, S., 1997. On the nucleation and propagation of phase transformation fronts in a NiTi alloy. Acta Mater. 45 (2), 683–700.

Shaw, J.A., Kyriakides, S., 1998. Initiation and propagation of localized deformation in elasto-plastic strips under uniaxial tension. Int. J. Plasticity 13, 837–871.

Sun, Q.P., Zhong, Z., 1999. An inclusion theory for the propagation of martensite band in NiTi shape memory alloy wires under tension. Int. J. Plasticity.

Timoshenko, S.P., Goodier, J.N., 1970. Theory of Elasticity. McGraw-Hill, New York.